



NAVAL POSTGRADUATE SCHOOL

MONTEREY, CALIFORNIA

THESIS

**ANALYSIS OF DEAD TIME AND IMPLEMENTATION OF
SMITH PREDICTOR COMPENSATION IN TRACKING
SERVO SYSTEMS FOR SMALL UNMANNED AERIAL
VEHICLES**

by

Thomas James Brashear, Jr.

December 2005

Thesis Advisor:
Co-Advisor:

Isaac I. Kaminer
Vladimir N. Dobrokhodov

Approved for public release; distribution is unlimited

THIS PAGE INTENTIONALLY LEFT BLANK

REPORT DOCUMENTATION PAGE

Form Approved OMB No. 0704-0188

Public reporting burden for this collection of information is estimated to average 1 hour per response, including the time for reviewing instruction, searching existing data sources, gathering and maintaining the data needed, and completing and reviewing the collection of information. Send comments regarding this burden estimate or any other aspect of this collection of information, including suggestions for reducing this burden, to Washington headquarters Services, Directorate for Information Operations and Reports, 1215 Jefferson Davis Highway, Suite 1204, Arlington, VA 22202-4302, and to the Office of Management and Budget, Paperwork Reduction Project (0704-0188) Washington DC 20503.

1. AGENCY USE ONLY (Leave blank)	2. REPORT DATE December 2005	3. REPORT TYPE AND DATES COVERED Master's Thesis
4. TITLE AND SUBTITLE: Analysis of Dead Time and Implementation of Smith Predictor Compensation in Tracking Servo Systems for Small Unmanned Aerial Vehicles		5. FUNDING NUMBERS
6. AUTHOR(S) Thomas James Brashear, Jr.		
7. PERFORMING ORGANIZATION NAME(S) AND ADDRESS(ES) Naval Postgraduate School Monterey, CA 93943-5000		8. PERFORMING ORGANIZATION REPORT NUMBER
9. SPONSORING /MONITORING AGENCY NAME(S) AND ADDRESS(ES) N/A		10. SPONSORING/MONITORING AGENCY REPORT NUMBER
11. SUPPLEMENTARY NOTES The views expressed in this thesis are those of the author and do not reflect the official policy or position of the Department of Defense or the U.S. Government.		
12a. DISTRIBUTION / AVAILABILITY STATEMENT Approved for public release; distribution is unlimited		12b. DISTRIBUTION CODE
13. ABSTRACT (maximum 200 words)		
<p>Recent advances in technology have allowed for Small Unmanned Aerial Vehicles (SUAVs) to employ miniaturized smart payloads such as gimbaled cameras, deployable mechanisms, and network sensors. Gimbaled video camera systems, designed at NPS, use two servo actuators to command line of sight orientation via serial controller while tracking a target and is termed Visual Based Target Tracking (VBTT). Several Tactical Network Topology (TNT) experiments have shown high value of this new payload but also revealed inherent delays that exist between command and actuation of the pan-tilt servo actuators controlling the camera. Preliminary analysis shows that these delays are due to a communication lag between the ground control station and the onboard serial controller, a data processing delay within that controller, and the mechanical delays of the gimbal. This thesis applies system identification techniques to the servo controller system and considers the implementation of a Smith Predictor into the camera control algorithm in order to reduce the overall effect of the lag on the system performance.</p>		
14. SUBJECT TERMS Small Unmanned Aerial Vehicle, Vision-Based Target-Tracking, Dead-time Compensation, Smith Predictor, System Identification		15. NUMBER OF PAGES 57
16. PRICE CODE		
17. SECURITY CLASSIFICATION OF REPORT Unclassified	18. SECURITY CLASSIFICATION OF THIS PAGE Unclassified	19. SECURITY CLASSIFICATION OF ABSTRACT Unclassified
20. LIMITATION OF ABSTRACT UL		

NSN 7540-01-280-5500

Standard Form 298 (Rev. 2-89)
Prescribed by ANSI Std. Z39-18

THIS PAGE INTENTIONALLY LEFT BLANK

Approved for public release; distribution is unlimited

**ANALYSIS OF DEAD TIME AND IMPLEMENTATION OF SMITH
PREDICTOR COMPENSATION IN TRACKING SERVO SYSTEMS FOR
SMALL UNMANNED AERIAL VEHICLES**

Thomas J. Brashear, Jr.
Lieutenant, United States Navy
B.S. Biological Systems Engineering, Texas A&M University, 1999

Submitted in partial fulfillment of the
requirements for the degree of

MASTER OF SCIENCE IN MECHANICAL ENGINEERING

from the

NAVAL POSTGRADUATE SCHOOL
December 2005

Author: Thomas James Brashear, Jr.

Approved by: Dr. Isaac I. Kaminer
Thesis Advisor

Dr. Vladimir N. Dobrokhodov
Co-Advisor

Dr. Anthony J. Healey
Chairman, Department of Mechanical and
Astronautical Engineering

THIS PAGE INTENTIONALLY LEFT BLANK

ABSTRACT

Recent advances in technology have allowed for Small Unmanned Aerial Vehicles (SUAUs) to employ miniaturized smart payloads such as gimbaled cameras, deployable mechanisms, and network sensors. Gimbaled video camera systems, designed at NPS, use two servo actuators to command line of sight orientation via serial controller while tracking a target and is termed Visual Based Target Tracking (VBTT). Several Tactical Network Topology (TNT) experiments have shown high value of this new payload but also revealed inherent delays that exist between command and actuation of the pan-tilt servo actuators controlling the camera. Preliminary analysis shows that these delays are due to a communication lag between the ground control station and the onboard serial controller, a data processing delay within that controller, and the mechanical delays of the gimbal. This thesis applies system identification techniques to the servo controller system and considers the implementation of a Smith Predictor into the camera control algorithm in order to reduce the overall effect of the lag on the system performance.

THIS PAGE INTENTIONALLY LEFT BLANK

TABLE OF CONTENTS

I.	INTRODUCTION.....	1
A.	OVERVIEW	1
B.	MOTIVATION	1
C.	STATEMENT OF THE REAL-TIME TRACKING PROBLEM	1
D.	OBJECTIVES	2
II.	BACKGROUND	5
A.	OVERVIEW OF TACTICAL NETWORK TOPOLOGY (TNT) EXPERIMENTS	5
B.	TRACKING TASKS AND PLATFORMS.....	5
1.	Telemaster UAV – Real-Time Vision-Based Tracker	5
2.	Rascal UAV – Real Time Pointer	6
3.	Antenna – Ground Based Pointer	8
C.	FEATURES OF VISUAL-BASED TARGET TRACKING (VBTT) AND POINTING.....	10
1.	Features of VBTT System	10
2.	Features of the Pointing Application.....	13
III.	APPROACH	15
A.	SYSTEM IDENTIFICATION.....	15
1.	Overview	15
2.	Assumptions	15
3.	Procedure.....	16
a.	<i>Gimbaled Camera System Onboard Telemaster UAV</i>	16
b.	<i>Video Pointer Antenna</i>	17
B.	DEAD RECKONING	20
C.	DEAD-TIME COMPENSATION (DTC)	21
1.	Overview of techniques.....	21
2.	Implementation of Smith Predictor	23
IV.	RESULTS AND DISCUSSION	25
A.	GENERAL OVERVIEW	25
B.	EVALUATION OF TRACKING PERFORMANCE IN A LABORATORY	25
1.	Analysis of Telemaster Gimbaled Camera Control System	25
2.	Results from 3DM Integration into Video Pointer Antenna.....	29
V.	CONCLUSION AND RECOMMENDATIONS.....	33
A.	CONCLUSION	33
B.	RECOMMENDATIONS.....	33
APPENDIX	BLOCK ALGEBRA OF DTC ADDITION.....	35
LIST OF REFERENCES	37	
INITIAL DISTRIBUTION LIST	39	

THIS PAGE INTENTIONALLY LEFT BLANK

LIST OF FIGURES

Figure 1.	Qualitative Representation of Equation 1.1 (from Reference [12]).....	3
Figure 2.	Modified Senior Telemaster UAV with Gimbal Detail.....	5
Figure 3.	Digital Servo Actuator and Serial Servo Controller (SSC-32).....	6
Figure 4.	Gimbaled System Onboard Rascal UAV a) side – cutaway b) front.....	7
Figure 5.	Schematic of Video Pointer Antenna.....	9
Figure 6.	Video Antenna Pointer Architecture.....	10
Figure 7.	Visual Based Target Tracking (VBTT) Architecture.....	12
Figure 8.	Control and Guidance Architecture.....	13
Figure 9.	Telemaster Gimbal System ID and Implementation Outline.....	16
Figure 10.	Camera FOV in PerceptiVU software unlocked (left) and locked (right).....	17
Figure 11.	Camera Focal Length and Field of View.....	18
Figure 12.	Degradation of the Effective Sampling Rate (From Reference [2]).....	19
Figure 13.	Adaptive Dead Reckoning (DR) Algorithm.....	21
Figure 14.	Smith Predictor (from Reference [11]).....	23
Figure 15.	Smith Predictor Implementation.....	24
Figure 16.	Resulting Smith predictor parameters.....	25
Figure 17.	Smith predictor effects on dead-time.....	26
Figure 18.	Delays Examined a) 0.001s b) 0.01s c) 0.0665s d) 0.1s.....	28
Figure 19.	Phase versus Delay relationship.....	29
Figure 20.	Graphical representation of observed delay of 3DM.....	30

THIS PAGE INTENTIONALLY LEFT BLANK

LIST OF TABLES

Table 1.	Observed 3DM delays as a function of read buffer size.....	31
----------	--	----

THIS PAGE INTENTIONALLY LEFT BLANK

LIST OF ACRONYMS

AMT	Automatic Motion Tracking
AP	Auto Pilot
ATT	Automatic Target Tracking
COTS	Commercial Off-The-Shelf
CIRPAS	Center for Interdisciplinary Remotely-Piloted Aircraft Studies
DCS	Digital Control System
DR	Dead Reckoning
DTC	Dead-time Compensator
EMI	Electro-Magnetic Interference
FLIR	Forward Looking Infra-red
FOLPD	First Order Lag Plus Delay
FOV	Field of View
GCS	Ground Control Station
GNC	Guidance Navigation and Control
GPS	Global Positioning System
LOS	Line of Sight
NPS	Naval Postgraduate School
PID	Proportional-Plus-Integral-Plus-Derivative
PWM	Pulse Width Modulation
RF	Radio Frequency
SI	Serial Interface
STAN	Surveillance and Target Acquisition
SUAV	Small Unmanned Aerial Vehicle
TNT	Tactical Network Topology
UDP	User Datagram Protocol
VBTT	Vision-Based Target Tracking

THIS PAGE INTENTIONALLY LEFT BLANK

ACKNOWLEDGMENTS

I want to thank my wife, Christine, for supporting me in all my endeavors while stationed here in Monterey. Your immeasurable support and encouragement were truly appreciated. You were always in my corner, and all the while completing a thesis of your own! You are beyond doubt an extraordinary woman and I am so lucky to have you as my wife – I love you Kickers!

I would also like to thank my family for their support. Mom, Dad, Connie, and Jay, thanks for unwavering support. Thanks also goes to Sean, I don't know what I would do without you Lil' Bro'!

I would like to express sincere thanks to Dr. Vladimir Dobrohodov for his relentless guidance throughout this thesis experiment. The success I achieved can only be attributed to the countless explanations that I received from him. It was a pleasure working for him. Thanks also to Dr. Kevin Jones who is the man behind all those mechanical systems – I learned a great deal from you.

I would also like to thank Dr. Isaac Kaminer for his supervision throughout my time here at NPS. As an instructor, he was excellent; as an advisor, his steadfast willingness to explore problems opened my eyes; but most importantly, as a friend he made my tour at NPS invaluable. It was due to his tutelage that I was able to persevere.

One more bunch of thanks goes out to Dani, Cindy, Jimmy, and Rip. Without you guys, I wouldn't have been able to have such a phenomenal time here in California. You afforded me the opportunity that helped maintain balance in my life. This stability was urgently needed, as the pressures of graduate work were quite immense – thank you.

THIS PAGE INTENTIONALLY LEFT BLANK

I. INTRODUCTION

A. OVERVIEW

As the ability to communicate on a global scale becomes more commonplace, systems with high reliability, ease of use, and minimized response time are needed to maintain a technological advantage. The use of Unmanned Systems has employed the benefits of such reliable communications while greatly evolving worldwide war-fighting capabilities. Specifically, Unmanned Aerial Vehicles (UAVs) were developed for surveillance and reconnaissance missions. They produce surveillance imagery from synthetic aperture radar, a forward looking infra-red (FLIR) and video cameras which can be distributed in real-time both to the front line soldier and to the operational commander, or even worldwide in real-time via satellite communication links. This vital advancement relies immeasurably on the speed and accuracy of the information being sent over these technological links. Because of the importance implicitly placed on the speed and accuracy of these systems, it is imperative that the underpinning mechanisms, required to create such systems, are worked out to maximize efficiency.

B. MOTIVATION

In Digital Control Systems (DCS), the transmission of command signals takes a finite amount of time to reach and be executed by its intended actuators. This inherent lag can make effective control of such time delayed systems difficult and potentially introduce error into that system. To address this characteristic of any DCS, a detection of this lag not only promotes a better understanding of the DCS, but it also becomes the preliminary step in the compensation of that delay.

C. STATEMENT OF THE REAL-TIME TRACKING PROBLEM

The gimbaled video camera system onboard the Small Unmanned Aerial Vehicles (SUAVs) developed at Naval Postgraduate School (NPS) is operated by two servo actuators which control the pitch (θ) and yaw (ψ) degrees of freedom of the camera's line of sight (LOS). This system, a component of the Visual Based Target Tracking (VBTT)

system, has three inherent delays that contribute to a decrease in the speed, accuracy and precision of the system as a whole; a communication lag between the ground control station and the onboard serial controller, a data processing delay within that controller, and the mechanical delays of the gimbal comprise the delay makeup. Two of these delays addressed in this study are the mechanical delays of the gimbaled system combined with the servo actuators and the processing delay of the serial controller used to coordinate the stream of commands from the computer running the control algorithm. The communication lag element was determined to independent of the other two and was seen as “unmanageable” with this approach. This thesis examines these delays in attempt to implement a compensation scheme.

D. OBJECTIVES

The NPS SUAV program goal is to provide a UAV equipped with Commercial off-the-shelf (COTS) sensors to serve as a surveillance and reconnaissance platform. Unlike the current UAVs used in military applications of today, the SUAV boasts a reduced price tag while maintaining the same capability to augment the common operating environment and situational awareness of the front line battle force further reducing the potential for individual harm.

The Visual-Based Target Tracking (VBTT) system onboard the SUAV utilizes a filtering solution to estimate the position of a visible target. This filtering solution relies on the ability to estimate the turn rate of the LOS connecting the UAV and target. This capability makes position estimation possible through the following kinematic relationship for the turn rate of the LOS (λ_{LOS})

$$\lambda_{LOS} = \frac{\bar{V}_p}{\rho} \quad 1.1$$

where \bar{V}_p is a linear velocity vector of the aircraft and ρ is the range from the aircraft to the target. This relationship’s feasibility is due to an assumption made that the ground speed vector of the UAV, V_g , can be controlled by the guidance algorithm [11] in such a way to be tangent to the line of sight (LOS) to the target; $V_p = V_g$. The difference

between these vectors is termed the guidance error, η . The control law employed in the VBTT guidance algorithm drives the value of η to zero. This concept, pictured in Figure 1, shows that by accomplishing the task, flight path takes the shape of an orbit above the center of the target.

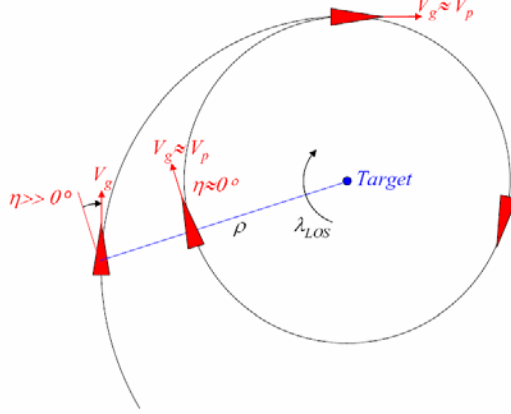


Figure 1. Qualitative Representation of Equation 1.1 (from Reference [12]).

The delays presented in the above problem statement affect the performance of this filtering technique. Accordingly, these delays will be the focus of this thesis. First, the lags are modeled in order to identify and quantify them. Next, system identification techniques are used to model the delays in the gimbaled controller. Then, the identified delays are balanced through the implementation of a dead-time compensator (DTC). The ultimate goal is to reduce the dead-time of the system in order to improve the tracking performance of the VBTT system. Finally, the implementation of the same tracking algorithm into a simple “target pointing” unit allows for a very effective solution for high gain antenna placement.

THIS PAGE INTENTIONALLY LEFT BLANK

II. BACKGROUND

A. OVERVIEW OF TACTICAL NETWORK TOPOLOGY (TNT) EXPERIMENTS

The Tactical Network Topology (TNT) field experimentation program is a cooperative effort between the Naval Postgraduate School (NPS), USSOCOM and its component commands. This program, a continuation of the Surveillance and Target Acquisition (STAN) program, conducts quarterly field experiments at the Center for Interdisciplinary Remotely-Piloted Aircraft Studies (CIRPAS) facility located at McMillan Field in Camp Roberts, CA. Its focus is the exploration of network-based warfare capabilities and their integration into current real-world occurrences.

B. TRACKING TASKS AND PLATFORMS

1. Telemaster UAV – Real-Time Vision-Based Tracker

The NPS's tracking SUAV is a Senior Telemaster RC aircraft that was modified to meet payload requirements. Seen in Figure 2, its main cargo is a gimbaled video camera system that is the initiation point of the Visual Based Target Tracking System (VBTT). Once airborne, this aircraft is either in autonomous navigation mode (standard mode provided by Piccolo Plus Auto Pilot (AP)) or it might be controlled via wireless RF link from the ground control station (GCS) for various specific missions. Using a traditional inner-outer loop control scheme, flight dynamics are managed by the onboard avionics system via the inner loop while aircraft navigation and target of interest orbiting are controlled from the GCS.



Figure 2. Modified Senior Telemaster UAV with Gimbal Detail.

The onboard gimbal is capable of carrying two cameras. It is located between the forward landing gear, also shown in Figure 2, and utilizes two HITEC digital servo actuators to provide movement to the high resolution, low light, black and white/color camera. The servos utilized were the HITEC HS-5996TG (pan) and HS-5998TG (tilt). The range and centering was modified to optimize the resolution of the controller, and the dead-band width was minimized to maximize the pointing accuracy. The HITEC servos are *digital* which means they use an onboard micro-processor to convert a serial Pulse Width Modulation (PWM) signal into a servo position. Both servos are managed by a serial-to-PWM controller named the Serial Servo Controller (SSC-II) manufactured by Lynxmotion. This controller offers an 8-bit resolution that is needed when tracking moving targets in a camera frame (later modifications of gimbal employ more versatile 10-bit SSC controller). The video, captured with the onboard camera, is transmitted via an onboard 2.4 GHz omni-directional antenna through a high gain ground-based directional antenna (described on page 8) to the Automatic Target Tracking (ATT) system at the GCS.



Figure 3. Digital Servo Actuator and Serial Servo Controller (SSC-32).

2. Rascal UAV – Real Time Pointer

As stated in the TNT experiment overview, network-based warfare capabilities are the focus of its ongoing research partnership. Specifically, the Telemaster aircraft

must transmit surveillance video collected onboard to the GCS before it can be relayed to the established ITT mesh network that serves as the information conduit for the exercises.

The Rascal UAV is the second aircraft controlled via the same GCS. Unlike the Telemaster, its purpose is to maintain surveillance of a known target position, while the Telemaster UAV system provides near real-time target position estimation based on a filtering solution. It uses mesh network communication to receive GPS coordinates of a target of interest. These coordinates become the center of the aircraft's new orbital path as it flies at a predetermined radius and altitude, specified by the GCS, while orbiting around this target. The camera pointing algorithm uses the GPS position of the target and its own instantaneous position and orientation to calculate the correct pan and tilt angles of the gimbal in order to precisely point the camera at the target; this simple transformation from inertial to gimbal frame allows for the LOS inertial stabilization. The calculation algorithm represents a direct coordinate transformation of the target with respect to the aircraft's continually changing its position and orientation making it a real-time pointer which is algebraically shown below in Equation 2.1.

$$R_{LTP}^c = R_b^c R_{LTP}^b \left\| \bar{P}_t - \bar{P}_{UAV} \right\| \Rightarrow \begin{pmatrix} \theta_{LOS} \\ \psi_{LOS} \end{pmatrix} \quad 2.1$$

The pan and tilt angles of the camera (2.1), thus continuously aligning the LOS with the target.

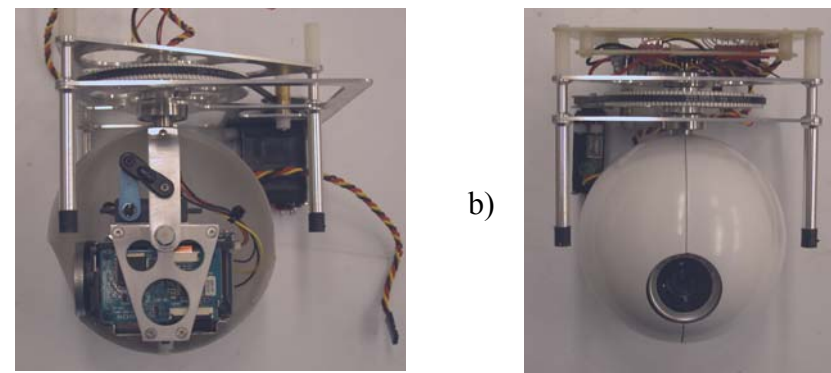


Figure 4. Gimbaled System Onboard Rascal UAV a) side – cutaway b) front.

The gimbaled system onboard the Rascal UAV, represents the second generation design and implementation. Pictured in Figure 4 above, it is powered by the same digital servos controlled by a newer SSC-32 10-bit controller providing better resolution than the previous SSC-II. The location of this system is also different than that of the Telemaster UAV. It is located halfway back on the bottom side of the fuselage. This positioning is aimed at precluding the landing gear wheel coming into view of the video image during operation. The camera also boasts improvements over the previous setup. Optical and digital zoom and color are among its additional features. Additionally, update rates of the controller are set at 20Hz even though GPS is updated once per second; a modified dead reckoning (DR) algorithm was implemented to estimate the UAV's position between the 1 Hz samples.

3. Antenna – Ground Based Pointer

Most of the RF links utilized throughout the TNT experiments could benefit from the accurate pointing of high-gain directional antennas. The video sent from the omni directional antenna onboard the Telemaster UAV is received at the GCS via a high gain directional antenna that is rotated with essentially the same above mentioned gimbaled system. The GCS video antenna, depicted in Figure 5, has the same two-axis gimbaled system that allows for pan and tilt commands. At this time they correspond to the azimuth and elevation required for the precise alignment of the LOS between the antenna and the targeted aircraft.

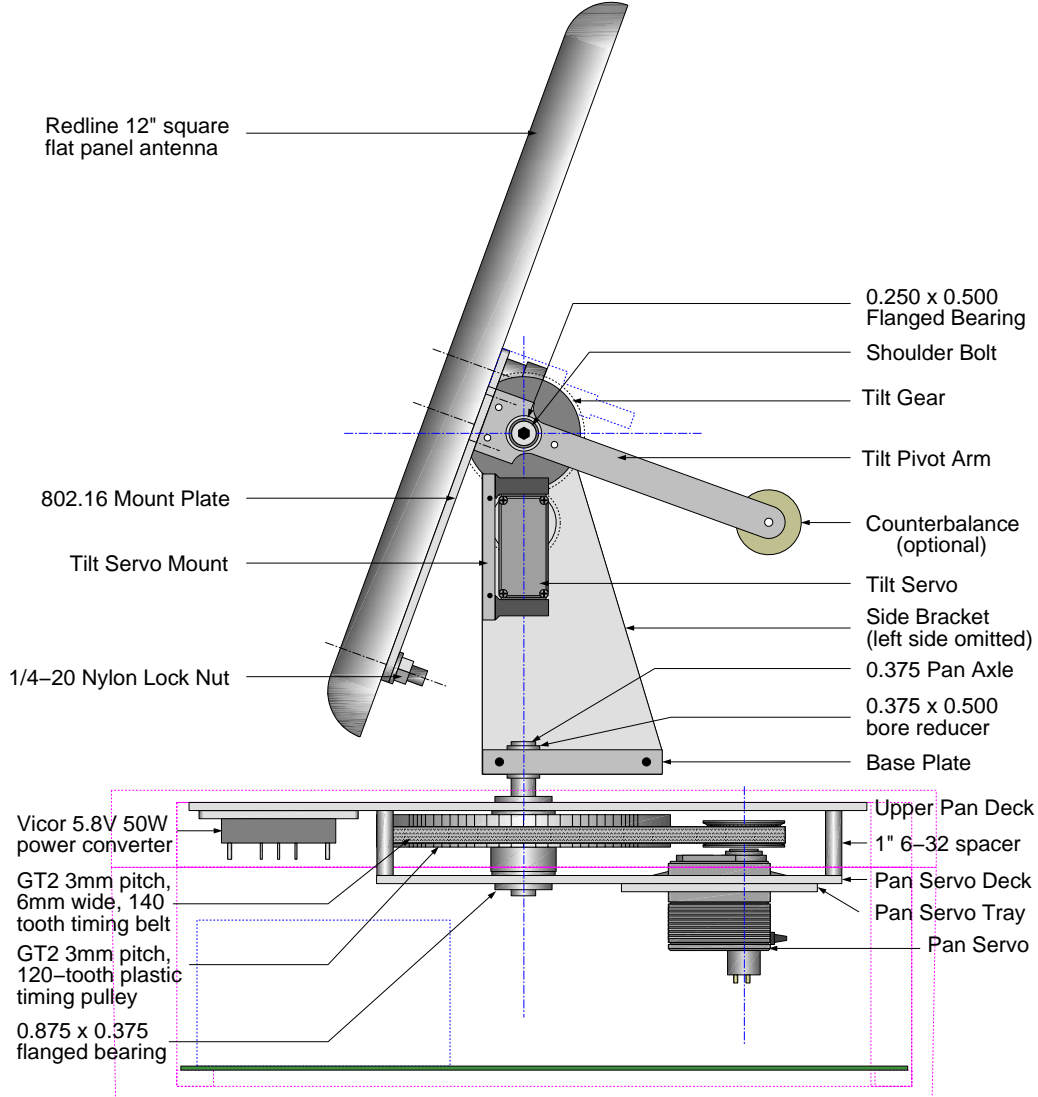


Figure 5. Schematic of Video Pointer Antenna.

As with the gimbaled camera systems, COTS equipment was used wherever possible to minimize the cost. The same digital servos employ the pan and tilt channels, again with the pan servo modified to allow for multiple revolutions. Typically, these servos can provide up to about 170° of proportional travel. In this case an SSC-II controller was used. The controller is just 8-bit, meaning at best there are just 256 possible servo positions. While this is fine for tilt ($\pm 45^\circ$ range – 0.35° resolution), for pan it is less than ideal ($\pm 180^\circ$ range, 1.41° resolution). This disadvantage is addressed in later antenna models, providing nearly 11-bit accuracy, or about 0.2° resolution. The

pointer antenna used a PC104 single-board computer from Win-Systems; model PPM-TX with a 266MHz processor. The PC included four serial ports and an Ethernet port. One serial port was used to control the servos, and the Ethernet port was used to connect the tracker to the host computer via User Datagram Protocol (UDP) connection. A schematic of the principal electronic elements and information flow of the pointer are shown in Figure 6.

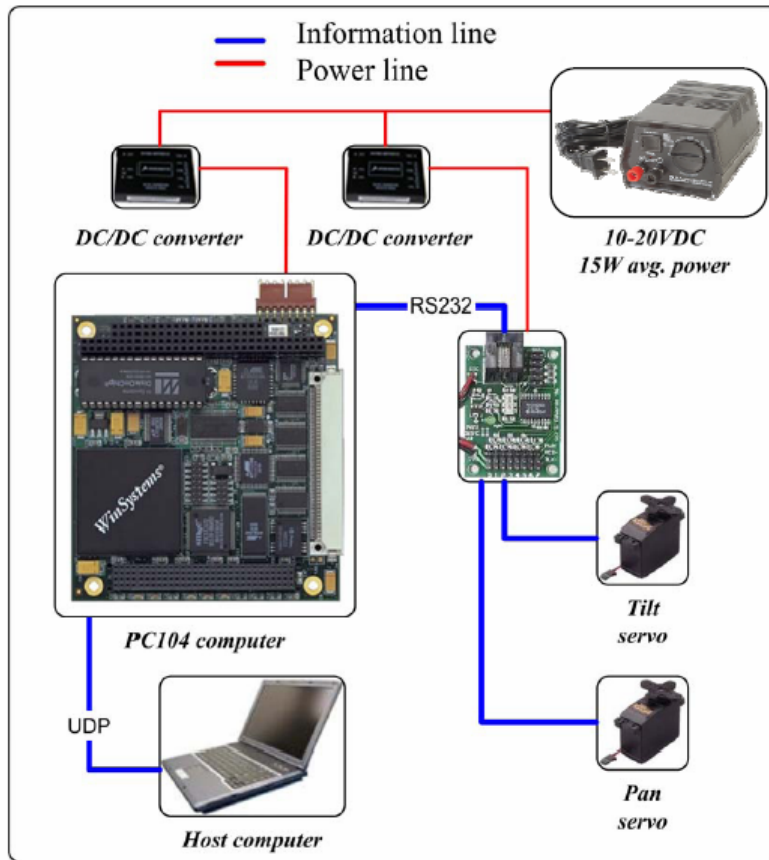


Figure 6. Video Antenna Pointer Architecture.

C. FEATURES OF VISUAL-BASED TARGET TRACKING (VBTT) AND POINTING

1. Features of VBTT System

Vision-Based Target Tracking (VBTT) is an emerging capability that would result in significant improvements of time on target and the ability to conduct detailed reconnaissance and provide simultaneous imagery. Ongoing development and flight

testing of an Automatic Target Tracking (ATT) and position estimation system are research interests within the TNT program. The system controls the UAV and the gimbaled camera system to maintain the centroid of the target identified by an operator in the center of the video image and provides an estimate of the target GPS position. The target can be stationary or moving. The VBTT system primarily addresses the following technological issues:

- Coupling of a vision-based object tracking capability with the guidance and control algorithms for small, low-cost UAVs.
- Development of guidance and control algorithms for vision-based tracking of a moving target.
- Development of small, light-weight, and low-cost gimbaled system using primarily COTS equipment for high speed, precision pointing in 3D space.
- Inertial stabilization of the LOS of the gimbaled system.
- Estimation of the moving target position and velocity based on passive vision data acquisition.

The VBTT system, shown in Figure 7, includes the modified Senior Telemaster UAV which acquires and transmits video via 2.4 GHz link to the ATT computer in real-time. During a mission, the operator of the ATT computer identifies the target of interest. The target appears inside of a small rectangle and is tracked by engaging the track mode. The position of the target in a camera frame is identified by the Cartesian coordinates of its centroid. This information is processed by the control algorithm, residing in the GCS, which sends guidance commands to the UAV and controls the camera to keep the target in the center of the video frame.

Three major components were developed and integrated into one system. The first element included a VBTT capability that used imagery provided by a gimbaled camera. Development of this module involved the design of a miniaturized gimbaled camera system, controller and integration of the ATT software developed by PerceptiVU, Inc [8]. Automated Motion Tracking (AMT) Software enables one to track an object in motion with a gimbaled camera as it moves within the camera frame. PerceptiVU allows

the user to select and lock on a target displayed on a GCS monitor. In the configuration used in this experiment PerceptiVU provides coordinates of the centroid of the selected target. These coordinates are then employed by the control and filtering algorithms introduced in the NPS ground station.

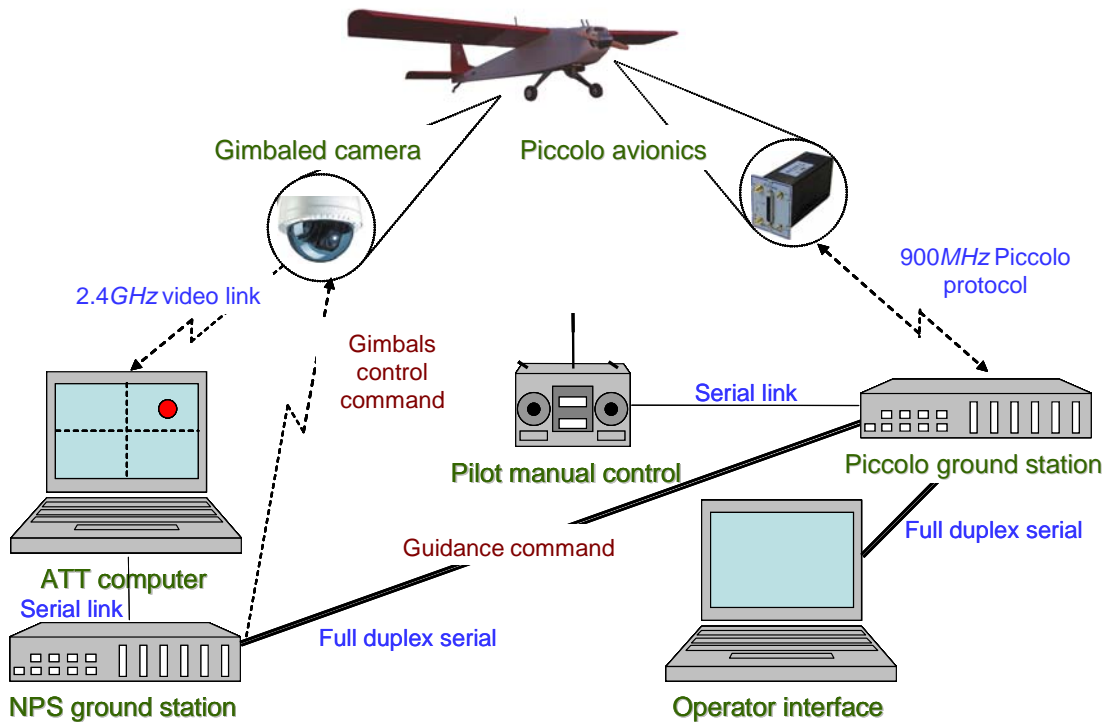


Figure 7. Visual Based Target Tracking (VBTT) Architecture.

The second component of the system includes the integrated UAV/camera control system. It contains several task-specific control loops for the UAV guidance, navigation and control (GNC) as well as for steering the gimbaled camera.

The GNC algorithm was designed to solve two principal tasks. First, it had to guide the UAV around the target while keeping the target in the camera frame. Second, it had to reduce the range estimation errors, coined Target Position Estimation, because the accuracy of the range estimation depends on the translational motion of the target in camera frame. The estimation error is minimized when the target moves parallel to the camera image plane.

Depicted in Figure 8, the control structure represents two distinct missions. The first one, when switch 1 is in the known target position, represents the mission of the pointing (“Rascal”) UAV. Alternatively, when switch 1 is placed to receive the estimated target position, the figure represents the mission of the tracking (“Telemaster”) UAV. Herein lays the ease for parallel technologies.

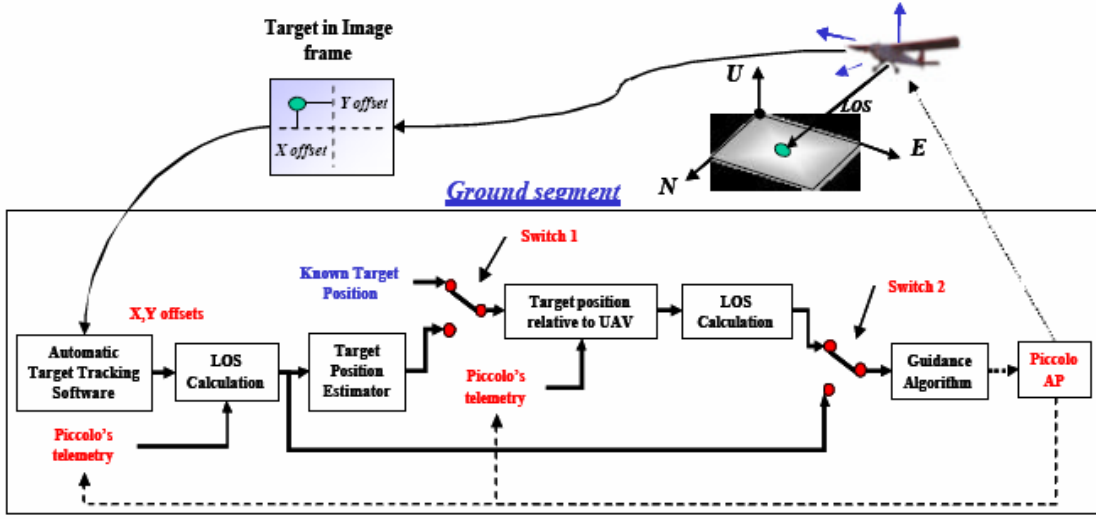


Figure 8. Control and Guidance Architecture.

2. Features of the Pointing Application

As mentioned previously, the directional pointing antenna takes on the same fundamental task as the Rascal UAV only applied to a slightly different set of initial conditions. First, the original setup has the roles reversed. In this case, the target is in motion and the gimbaled system is stationary. This is easily transferable as the original algorithm requires two position coordinates and attitude in order to compute the azimuth and elevation angles required for precise LOS orientation.

THIS PAGE INTENTIONALLY LEFT BLANK

III. APROACH

A. SYSTEM IDENTIFICATION

1. Overview

The results from several past TNT experiments combined with recent thesis work revealed inherent delays that exist within the VBTT system. Preliminary analysis connected these delays to the communication links, data processing time, and the mechanical delays innate to the design of the gimbaled system. It became necessary to model the overall system in order to quantify these delays so as to account for them. Then the modeled system could be used toward the compensation of the analyzed dead-time. Two laboratory experiments were established and conducted to ascertain these quantities; the system identification of the Telemaster gimbaled camera control system and the observation of delay experienced in the 3DM sensor.

The quality and precision of video acquired by the camera onboard the Telemaster UAV was directly connected to the success of its NPS-developed guidance and navigation (GNC) algorithm as well as its target position estimation solution. Since this relationship was pivotal to the mission of the Telemaster UAV, the gimbaled camera control system was modeled in the laboratory. An accurate representation of the process would confidently lead to a decreased system response time via compensation.

An introduction of additional sensors into the system contributed to the aforementioned delays. The addition of a solid state 3-axis (pitch, roll, and yaw) sensor to the video pointer antenna resolved orientation issues at startup (i.e. the need to orient the antenna to the north) and allowed for a mobile-based application for the “tracking” antenna. This successful implementation also laid the foundation for parallel advancement with the feature of an inertially-stabilized gimbaled camera system onboard the UAVs.

2. Assumptions

While conceptualizing up the experiment, the proposal to use visual feedback from the PerceptiVU software was made. The true processing speed of the PerceptiVU software was 30 Hz that is determined by the highest possible rate of the frame grabber

used (Matrox Meteor-II). This was a reasonable assumption because the relative difference between the anticipated delays of the 3DM sensor (slow update rate sensor due to the technology used [10]) and the visual feedback (fast update sensor) was assumed significant enough to measure. Furthermore, this assumption was believed to be transferable to the subsequent identification of the gimbaled system on the Telemaster UAV. Finally, since the results of the system identification would merely provide starting point from which to further improve through actual adjustment and tuning of the compensated system, this assumption was made and the visual feedback received was presumed immediate.

Two additional assumptions were made in the analysis. Since the communication delay mentioned earlier was not perceived as constant nor might be accurately modeled together with the gimbaled system, it was not considered during system identification. This communication lag, although directly affecting the system performance, was observed as an Electro-Magnetic Interference (EMI) issue. The final assumption dealt with the separation of the two gimbaled directions, pan and tilt. The proposed analysis assumed that the delays in each axis were independent and could be identified separately. This allowed for independent identification without the concern for a coupled system.

3. Procedure

a. Gimbaled Camera System Onboard Telemaster UAV

This laboratory experiment was established to accurately model the gimbaled camera control system. The experimental approach is outlined in Figure 9.

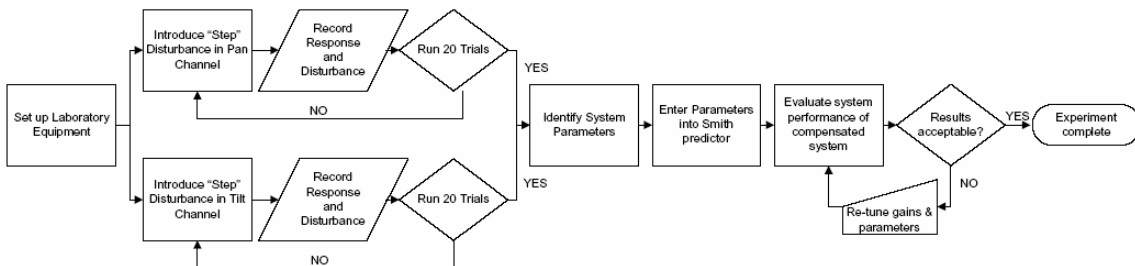


Figure 9. Telemaster Gimbal System ID and Implementation Outline.

The conceptual idea was to introduce a “step” disturbance to each axis independently and measure the response from the control system once initiated. The disturbance was introduced by locking onto a target within the FOV of the camera about 8° to 10° off of the origin of the camera frame. Figure 10, shows the view of the video as seen through the PerceptiVU software on the ATT computer. The left portion of the figure illustrates the “set up” portion of a trial whereas the right half of the figure shows the target acquired after the disturbance was introduced (note - yellow box = control system idle / red box = control system initiated). Approximately twenty trials for both pan and tilt directions were conducted. Next, the recorded data from these trials was analytically examined to determine the system parameters. Once identified, these parameters were introduced into the corresponding portions of the Smith Predictor that was added to the control loop. The original “step” disturbance was applied again to the system in order to re-tune system gains. Finally, the variation in system response due to the dead-time compensation was recorded and evaluated.

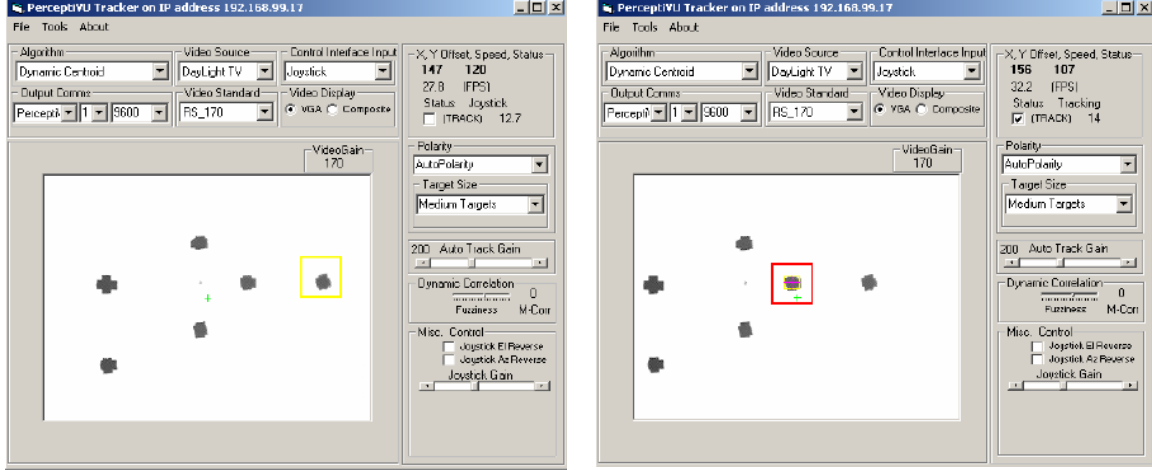


Figure 10. Camera FOV in PerceptiVU software unlocked (left) and locked (right).

b. Video Pointer Antenna

The experiment modeling the delay experienced by the 3DM sensor was also organized and conducted in the laboratory. The concept was to introduce a “step” disturbance to the base of pointer antenna and observe how the 3DM sensor measured that disturbance. The 3DM unit is a solid-state 3-axis pitch, roll, and yaw sensor. It

accomplished tilt sensing through orthogonal accelerometers and magnetic compass functions via orthogonal flux gate magnetometers. It supported a maximum output rate of approximately 30 Hz.

To achieve visual feedback, a small, fixed-aperture camera was affixed to the mount plate of the antenna. The antenna was positioned at proper focal distance from a whiteboard mounted to the wall such that the LOS of the camera was perpendicular to the whiteboard. The antenna was hinged to the table so that it could only be rotated about the y-axis. Next, the field of view (FOV) of the camera in this location was measured in inches and outlined on the whiteboard, detailed in Figure 11. The video from this camera was fed to the ATT computer through coaxial connection. The output from the PerceptiVU software was feed back to the PC104 running the antenna control algorithm via RS232 serial connection. Since the only measured quantities from this experiment were the output from the 3DM sensor and the visual feedback, the pointing control system was disabled. This ensured representative visual data was passed to the ATT. The data collection was established in real-time such that both PerceptiVU and 3DM data could be synchronized with time. This allowed for the analysis of the 3DM performance.

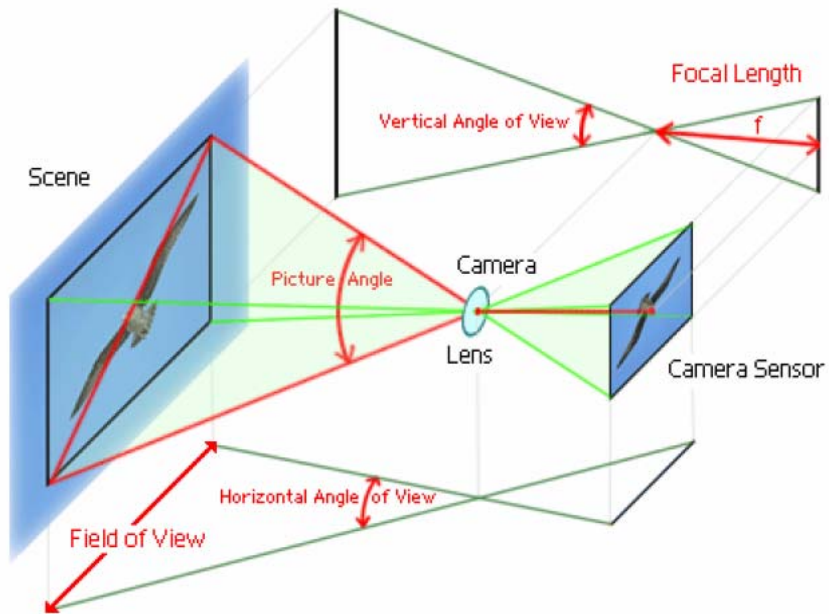


Figure 11. Camera Focal Length and Field of View.

The measured FOV and distance between the camera lens and the wall were used in the determination of the FOV of the camera in degrees as opposed to inches. These values were needed as conversion factors (from linear displacement to angular measure) to accurately model the system. The precision of these measurements was next examined. Using a standard measuring tape, the degree of accuracy was one sixteenth on an inch. Incorrect measurements could potentially introduce error into the calculation of the camera's FOV. Assuming the maximum degree of measurement error was less than ± 1 inch, the introduced error was examined within the following relationship

$$\theta_{FOV} = 2 \arctan\left(\frac{D}{2f}\right) \quad 3.1$$

where θ_{FOV} represents the FOV of the camera, in degrees, D is the distance of the FOV, in inches, and f is the focal length of the camera, in inches.

Due to the serial communication between the 3DM and the PC104, it was also necessary to evaluate the effect of the read buffer size on the performance. The problem of performance evaluation for the serial communication is twofold. On the one hand, the number of required internal loops necessary to process one package of raw data is a very explicit measure of the correctness of the serial interface (SI) tuning.

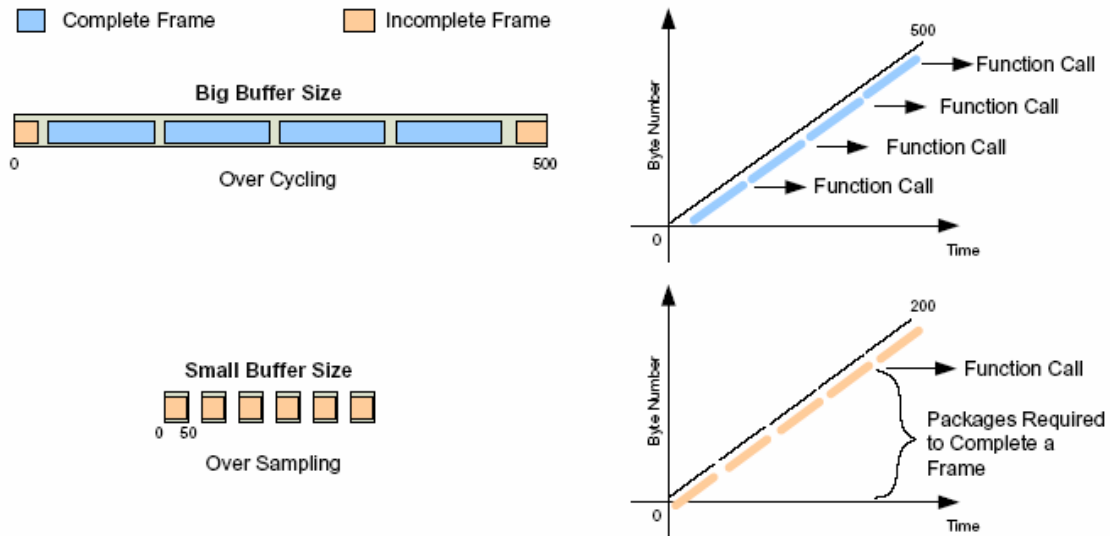


Figure 12. Degradation of the Effective Sampling Rate (From Reference [2]).

This means that if the frame length is much less than the package size, the parsing procedure will run multiple while-loops, thus extending the time load of the parsing routine. In contrast, despite the fact that all bytes are processed and multiple function calls are issued, triggering the next scaling procedure, the effective sampling rate delivered by the parser will be lower than the original sampling rate of the sensor, shown in Figure 12. Similarly, if the amount of bytes delivered at once to the parser is much less than the frame length, then the parser will require several runs to collect enough bytes for one complete frame [2]. It will also decrease the effective sampling rate of the SI. Accordingly, buffer sizes of 64 and 1024 bytes were introduced to examine performance.

To start the assessment, the algorithm was initiated and the antenna unit was rotated approximately -5° about the y-axis and then released. This “fall” of the unit back to the horizontal LOS of the camera with the whiteboard approximated the step disturbance. Approximately twenty trials were performed to account for the possibility of outliers. The “step” disturbance could now be plotted together with the corresponding data from the 3DM. Graphical analysis would expose the time delay and the time constant associated with the integration of this sensor into the pointer antenna allowing for compensation of initial angular orientation.

B. DEAD RECKONING

As mentioned previously, the slow update rate of GPS data combined with the possibility of communication lags and frequency confliction showed the need for dead reckoning algorithm to be added to the control scheme. This would allow the system under consideration to advance target position based on the last updated velocity and attitude information.

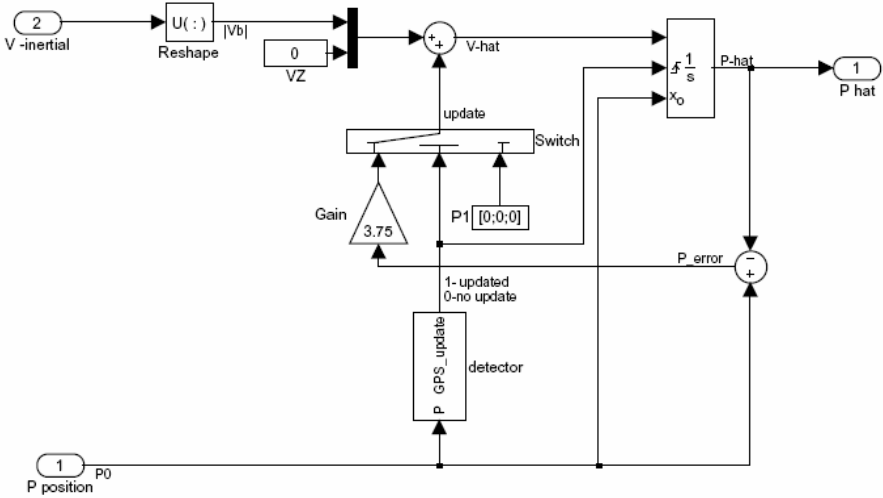


Figure 13. Adaptive Dead Reckoning (DR) Algorithm.

Figure 13 shows a SIMULINK diagram which represents the algorithm incorporated into the control scheme. It takes the last known inertial velocities and integrates them to get an estimated position. Under normal operation with an accurate GPS message, a positional vector of $[0; 0; 0]$ is added to the incoming velocities and the estimate passes through the logic, thus unaffected the outcome. On the other hand, if the GPS_updater subsystem is triggered, then the error between the last known true and estimated position is used to compensate for the accumulated error. This DR logic allows the system to continue pointing along the last known path with improved accuracy until a new GPS message is delivered. In the case of the ground pointer antenna, this feature, combined with the horizontal and vertical beam width of the antenna, will tolerate a noisier system and maintain a successful video link more consistently. The Rascal UAV will benefit from this algorithm in that it will use its own velocity and that of the target to successfully estimate the position in the event of a momentary loss of GPS.

C. DEAD-TIME COMPENSATION (DTC)

1. Overview of techniques

The dead-time introduced into the tracking system significantly deteriorates the system performance eventually causing a loss of target. Although the already present proportional-plus-integral (PI) controller can handle a small amount of dead-time, it exhibits poor performance when the system displays longer dead-time. Several methods

have been developed that address dead-time. Such techniques range from predictive controllers that minimize a cost function, to a compensator designed for servo applications called a Smith Predictor, to complex optimal controller design and direct synthesis methods most suitable for continuous systems [5]. Each of these methods was evaluated weighing their weaknesses versus returns of implementation into the gimbal control algorithm. The compensation technique chosen was proposed during the 1950's by O. J. M. Smith, subsequently named the Smith predictor.

The Smith predictor facilitates the removal of the time delay term in the closed loop characteristic equation [6]. This straightforward dead-time compensation (DTC) technique is the optimal controller for a delayed process for servo applications experiencing step disturbances often reducing the delay up to 30% [5]. The method is based on the idea that many higher order systems can be represented in first order lag plus time delay (FOLPD) form. The compensator requires the system identification of three modeled parameters: a time constant, a velocity gain, and a dead-time. Once identified, these parameters are inserted into their respective places in the compensated system. The final step of implementation would require a re-tuning of the scheme to maximize the performance of the system at hand. The simplicity of this technique combined with its suitability to the PI controller made it the most evident selection. Figure 14 shows a schematic of how a Smith Predictor is introduced to a system.

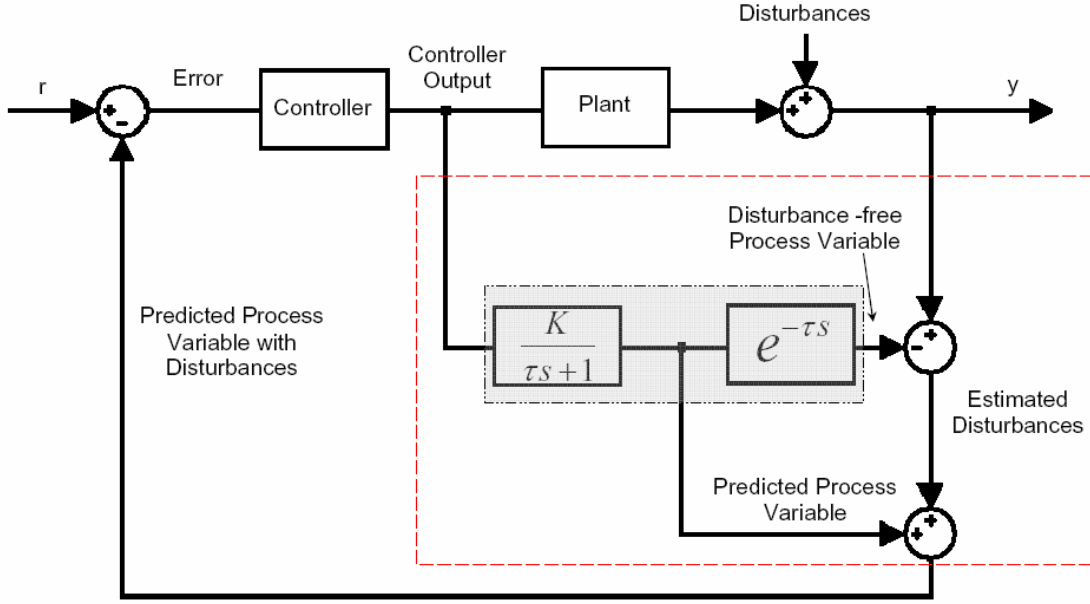


Figure 14. Smith Predictor (from Reference [11]).

The compensator consists of an inner loop that introduces two extra terms into the feedback path. Since its addition runs in parallel to the system and essentially represents the identified Plant, it does not affect the overall transfer function of the system (if system ID was correct); shown in the Appendix. The first part identified in the figure is the first box the shaded area which represents the dynamic first order system model. It takes controller output and estimates what the process variable would look like without any disturbances. This estimate term is added to the feedback path. The second part shown in the above figure is the second box in the shaded area which represents the time delay term. It is fed by the same controller input. This block outputs a delayed but otherwise unchanged signal. This delayed signal term is now subtracted from the feedback path, producing an estimate of the disturbances. This procedure allows the controller to determine “ahead of time” what the next control effort should be. The delay has been effectively moved out of the loop [11].

2. Implementation of Smith Predictor

The Smith predictor was convenient to introduce into the existing PI gimbal control scheme. As identified in Figure 14, the required terms were appropriately added and subtracted from the feedback path of the existing controller. Figure 15 shows the

SIMULINK model of the gimbal controller modified for the addition of the Smith predictor. Outlined in the green box is the gimbal first-order-approximation-model while the red box delineates the time delay block inserted. It is inside both of these blocks, that the parameters determined from the system identification will be included. Finally, shown in the dashed-line oval is a switch added to observe the performance of the system once tuned with the DTC as well as without the compensation. It also allowed for ease of maneuver between the compensated and non-compensated systems. The PI controller along with the tracking gains for both the pan and tilt channels were expected to be different depending on the status of the DTC.

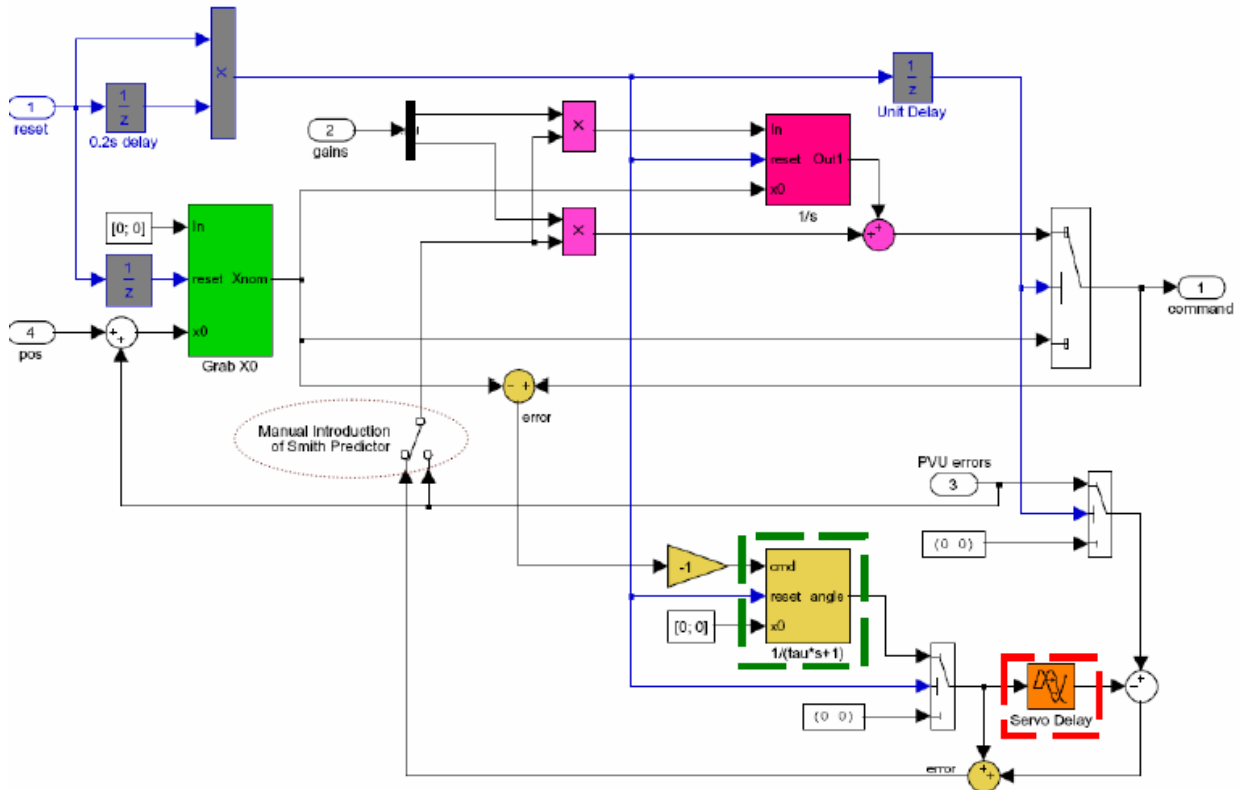


Figure 15. Smith Predictor Implementation.

IV. RESULTS AND DISCUSSION

A. GENERAL OVERVIEW

During the most recent TNT experiments, TNT 05-4 and 06-1, all gimbaled components performed well. The VBTT was successful in tracking both static and slow moving targets. Actual tracking time was increased twofold over the uncompensated controller experiments from the previous year. The position filtering solution convergence time also decreased substantially. When the UDP flow, which transmitted the GPS message to the PC104 inside the ground pointer antenna, periodically dropped out, the adaptive dead reckoning algorithm augmented the tracking by keeping accurate LOS orientation movement smooth with the SUAV in flight.

B. EVALUATION OF TRACKING PERFORMANCE IN A LABORATORY

1. Analysis of Telemaster Gimbaled Camera Control System

From the laboratory experiment, the system was modeled to arrive at the required parameters needed for the Smith predictor. The average time delay was accepted as 0.0665 sec. The time constant and gains referring to the dynamic system modeling are listed below in Figure 16.

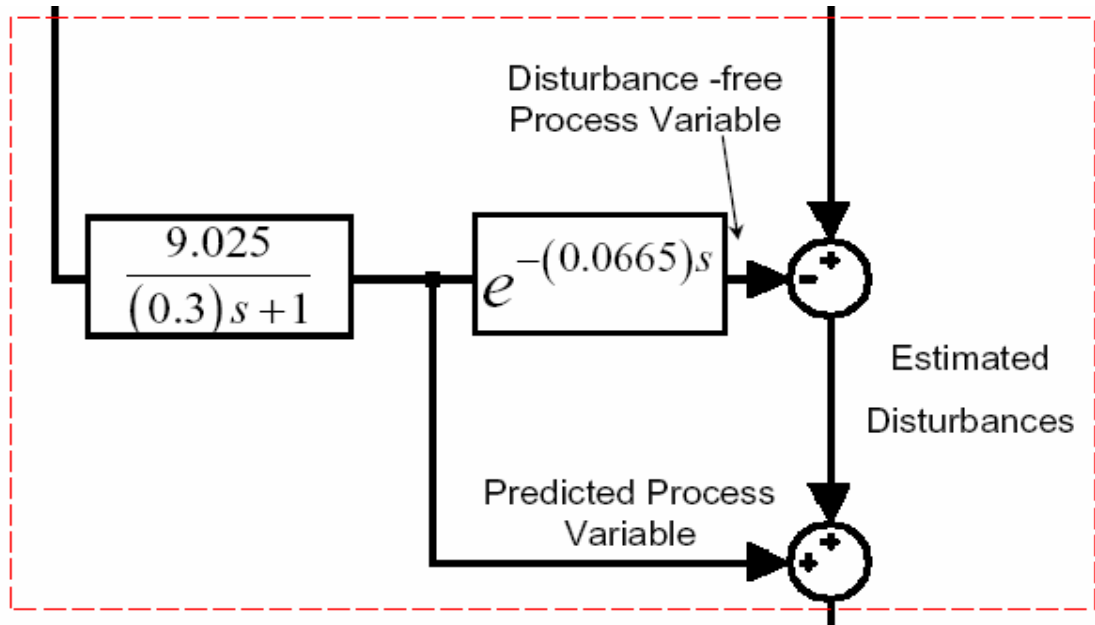


Figure 16. Resulting Smith predictor parameters.

The time delay was calculated by taking the average of all twenty experimental runs. Once this value was acquired, the gimbal command output was then approximated as a first order system through a curve-fitting technique. This first order system along with the calculated time delay were both placed back into the Smith predictor to measure its effectiveness. Twenty more experimental runs, that introduced the similar “step” disturbance, were conducted on the newly compensated system. The resulting command, feedback, and tracking status data were collected and plotted in Figure 17.

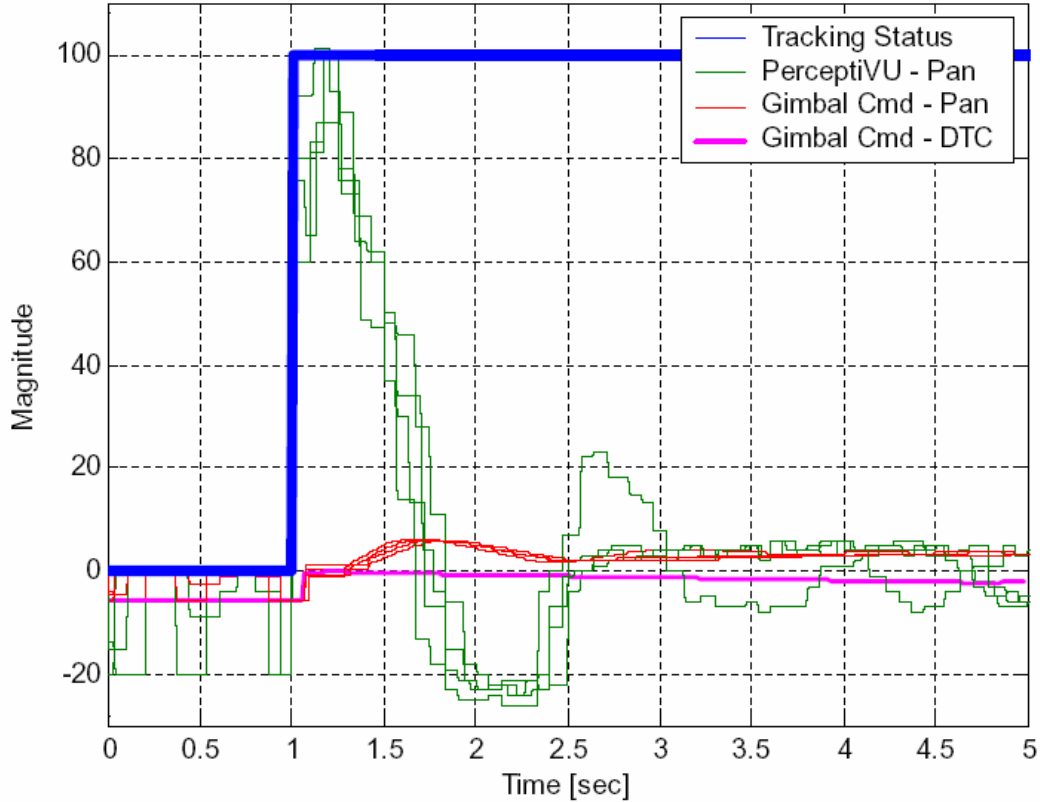


Figure 17. Smith predictor effects on dead-time.

Characterized by the thick magenta line, the average gimbal command after implementation of the Smith predictor shows a decrease of 0.0165s in system response. This difference between the uncompensated (red) and compensated (magenta) systems represents a 24.8% reduction in the dead-time of the system. These results corresponded fairly well to the advertised dead-time reduction of up to 30% when the Smith predictor

was used. Similar results were received for the tilt channel. Consequently, the decision was made to consider the two channels, pan and tilt, equal in response and use the same calculated parameters for each.

With this “initial guess” validated by positive results, it could now be adjusted to determine if a better performance of the real (vs. identified that is always “virtual”) unit existed. The same laboratory setup in the Telemaster portion of Chapter 3 was performed again, however, this time on a moving pendulum target. The use of a pendulum, which frequency of oscillations is fixed by its length, allows for precise measurement of phase shift between referenced and measured signals. This alteration was initiated so that phase or effectiveness of the incorporated delay could be measured. Since 0.0665 sec was the starting point from an average of the experimental trials; values on either side were examined in an attempt to optimize the delay value and tracking gains on a moving target. Of the several trials accomplished, four delay values were chosen to represent the range that experimentally exhibited a departure from the accepted performance of the system.

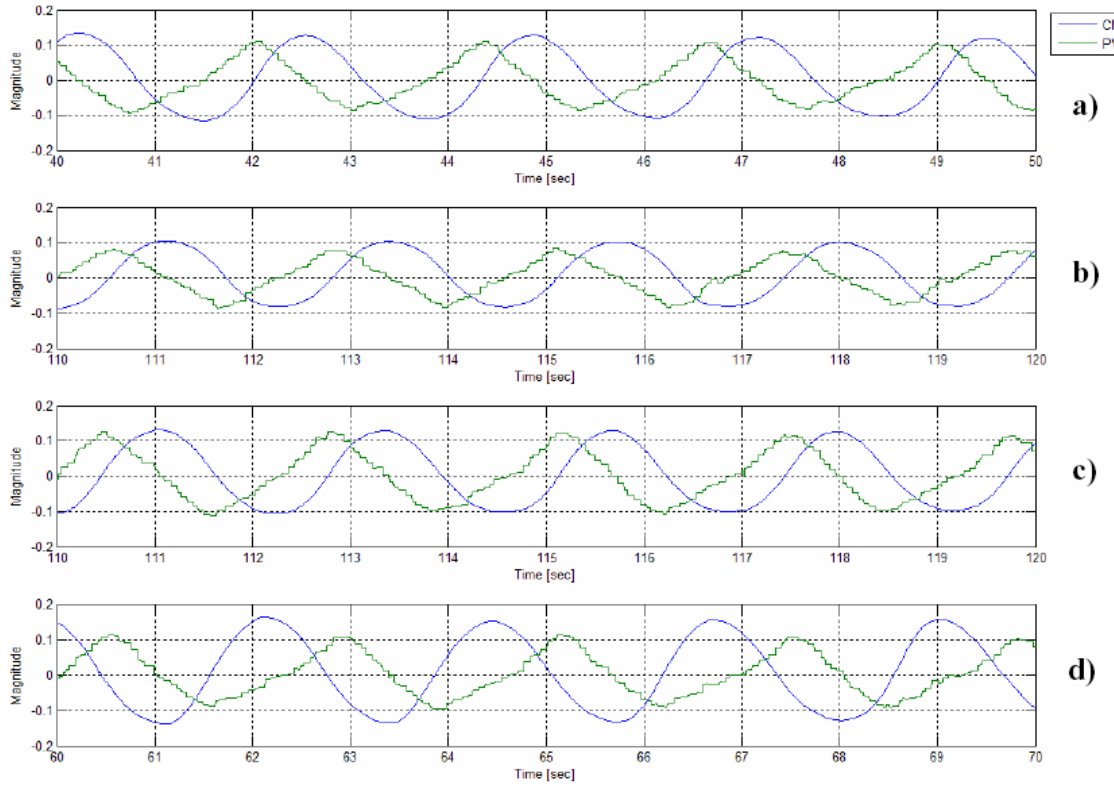


Figure 18. Delays Examined a) 0.001s b) 0.01s c) 0.0665s d) 0.1s.

Shown above is a graphical representation of how each of the investigated delays shifts the phase of the system's commanded response. The phases for these four delays were also represented on a semi-log plot in Figure 19. This relationship depicts a transitional point, conveniently occurring at the identified time delay of 0.0665 sec, where a larger value of delay will introduce an undesired effect on the system. To the left of this transitional point, it stands that smaller values of delay will allow the system to more closely follow the actual motion of the target while the contribution to a phase shift is minimized. This effectively increases the robustness of the system's performance.

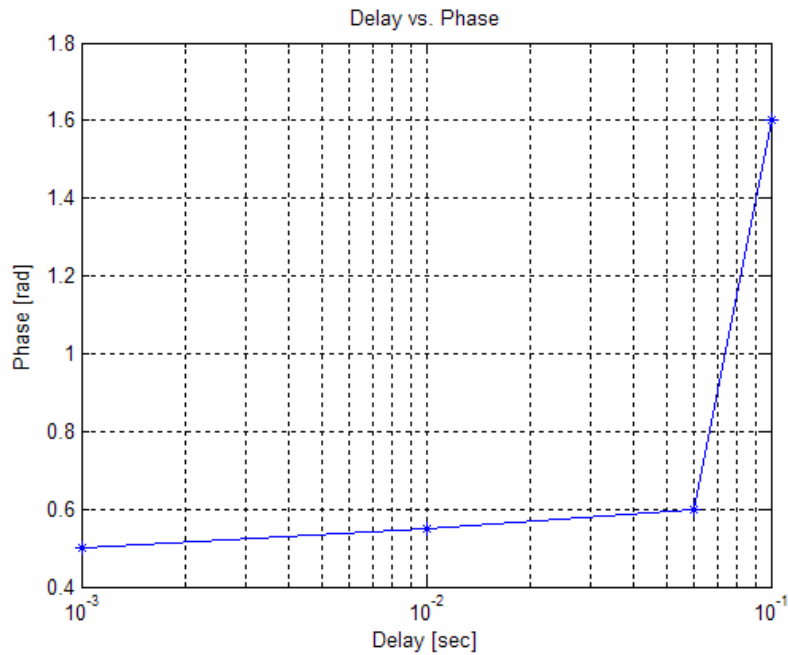


Figure 19. Phase versus Delay relationship.

2. Results from 3DM Integration into Video Pointer Antenna

The data, produced from one of the “step” disturbance introduction trials, is characterized in Figure 20. It shows the delayed response of the 3DM unit. Also illustrated here is the error introduced due to measurement error. This value was calculated to affect the output by no more than $\pm 0.37^\circ$, also represented in Figure 20 as a shift in the PerceptiVU output.

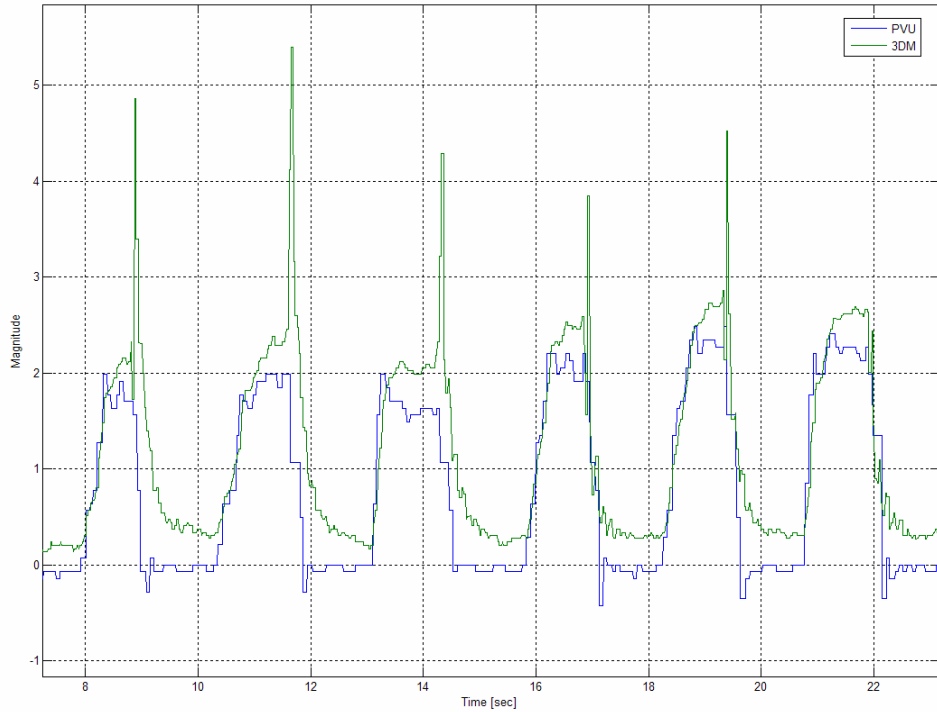


Figure 20. Graphical representation of observed delay of 3DM.

Due to the serial communication between the control algorithm on the internal PC104 and the 3DM, the results of the read buffer experiment are presented in Table 1. It compares the velocity gains and time delays between the responses from visual feedback and the 3DM sensor. This showed that the optimal read buffer size for the current 3DM driver was 64 bytes. The delay for 1024 byte read buffer more than doubled that observed by the 64 byte read buffer.

Cycle [#]	64 byte read buffer size			1024 byte read buffer size		
	V_{PVU} [°/sec]	V_{3DM} [°/sec]	δ_{LAG} [sec]	V_{PVU} [°/sec]	V_{3DM} [°/sec]	δ_{LAG} [sec]
1	-2.50090	-3.69350	0.034236153	-2.0664	-5.0558	0.070974576
2	-4.98180	-3.93200	0.036358464	-2.4846	-2.8312	0.085584416
3	-3.83750	-5.21950	0.059113150	-4.2476	-2.8312	0.057010622
4	-4.11200	-5.16960	0.029851190	-3.1211	-2.8312	0.173706897
5	-1.93290	-5.35530	0.059849655	-1.7429	-2.8312	0.014476276
6	-3.60190	-2.70480	0.053817760	-2.6358	-2.8312	0.068074123
7	-1.40370	-5.60650	0.058634223	-5.1997	-2.8312	0.087618891
Mean	-2.03370	-2.88011	0.030169145	-2.6873	-3.2840	0.069680725

Table 1. Observed 3DM delays as a function of read buffer size.

THIS PAGE INTENTIONALLY LEFT BLANK

V. CONCLUSION AND RECOMMENDATIONS

A. CONCLUSION

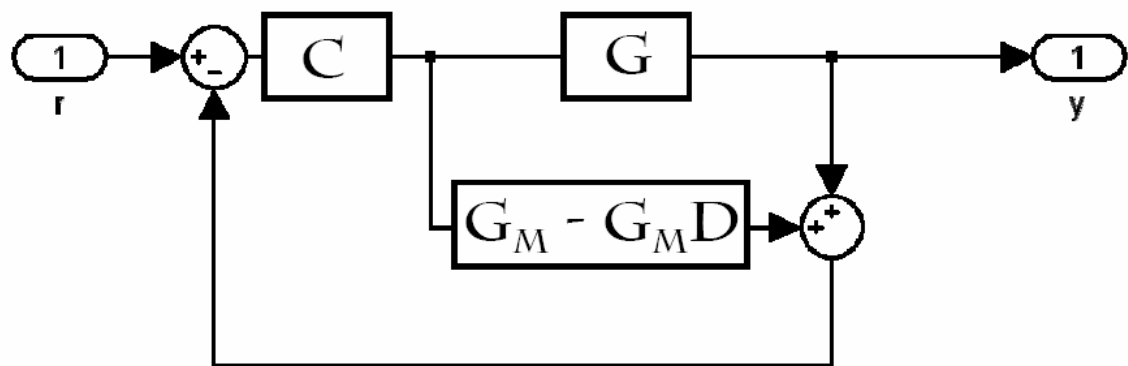
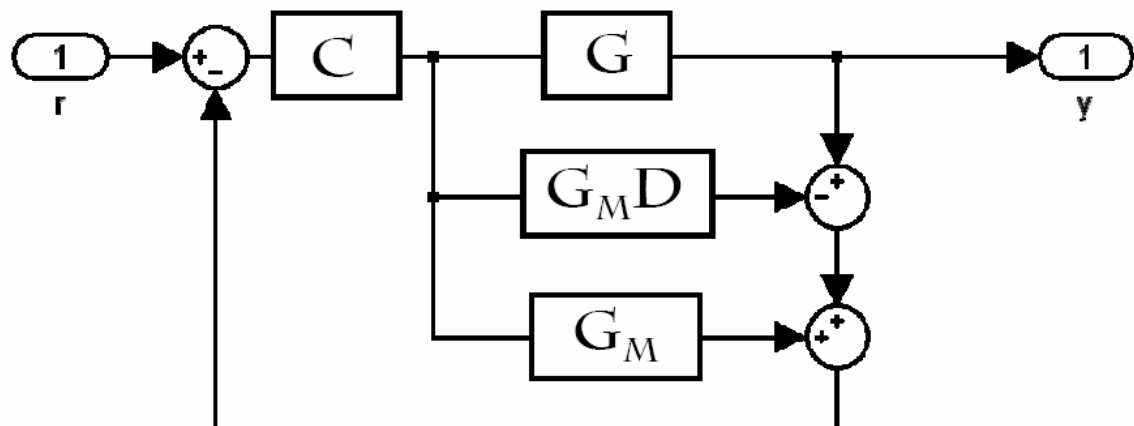
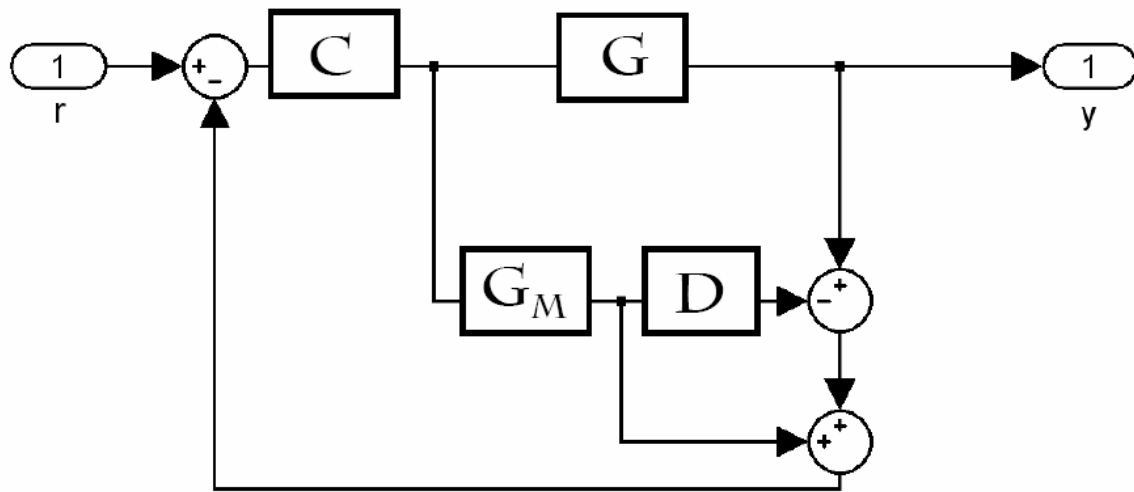
The introduction a Smith predictor dead-time compensation scheme greatly enhanced the performance of each of the systems examined. Nearly maximized, the 24.8% reduction allowed for a more robust tracking system on the Telemaster UAV. Target losses were drastically reduced, a more evenly transmitted video signal was received, and the target position filtering solution exhibited faster convergence times due to this implementation. An interesting relationship between the time delay and the phase delay of the command actuation presented itself when a moving pendulum target was examined. This connection exposed the range of effective delays useful in the DTC algorithm. Furthermore, through finer adjustments of tracking gains the tracking subsystem became more responsive. This concluded that the Smith predictor increased the robustness of the system.

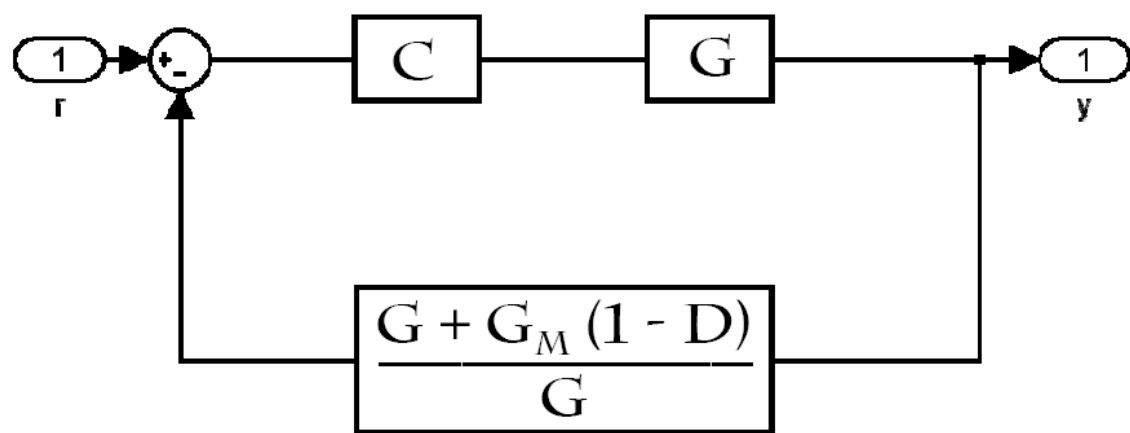
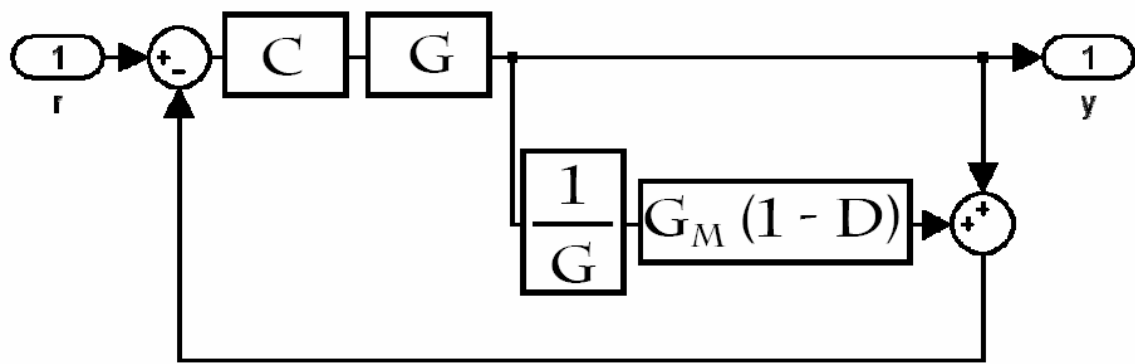
B. RECOMMENDATIONS

The precision and accuracy of the surveillance gimbaled camera system onboard the UAV is instrumental to the accuracy and speed of convergence of the target positioning filter. Because of this relationship, the VBTT system should be further examined to expose other possible errors prolonging position estimation convergence times and contributing to target losses. The cleaner the data entering the filters, the quicker the convergence time will become. Inertial stabilization of the camera's LOS as well as video stabilization will help advance towards that goal. Disturbance rejection could also facilitate these improvements.

THIS PAGE INTENTIONALLY LEFT BLANK

APPENDIX BLOCK ALGEBRA OF DTC ADDITION





$$\frac{y}{r} = \frac{CG + CG_M(1 - D)}{1 + CG + CG_M(1 - D)} \underset{\text{simplifying}}{\approx} \frac{CG_M}{1 + CG_M}$$

LIST OF REFERENCES

- [1] Ackerman, J. (2005). Error Analysis of Sensor Measurements in a Small UAV (Master's thesis, Naval Postgraduate School, 2005). *Master's Abstracts International*.
- [2] Dobrokhodov, V. N., & Lizarraga, M. (2005). Developing Serial Communication Interfaces for Rapid Prototyping of Navigation and Control Tasks. *American Institute of Aeronautics and Astronautics*. Retrieved November 28, 2005, from http://pdf.aiaa.org/preview/CDReadyMMST05_1088/PV2005_6099.pdf
- [3] Flood, C. H. (2001). Design and Evaluation of a Digital Flight Control System for the Frog Unmanned Aerial Vehicle (Master's thesis, Naval Postgraduate School, 2001).
- [4] Lizarraga, M. (2004). Autonomous Landing System for a UAV (Master's thesis, Naval Postgraduate School, 2004).
- [5] O'Dwyer, A., & Ringwood, J. (1999). A classification of techniques for the compensation of time delayed processes. Part 2. Structurally optimised controllers. *Modern Applied Mathematical Techniques in Circuits, Systems and Control*, 187-190. Retrieved November 28, 2005, from <http://www.dit.ie/DIT/engineering/csee/staff/aodwyer/research/files/paper99h.doc>
- [6] O'Dwyer, A., Snyder, J., & Heeg, T. *Dead-time compensators: performance and robustness issues*. Retrieved November 29, 2005, from <http://www.dit.ie/DIT/engineering/csee/staff/aodwyer/research/files/paper00c.pdf>
- [7] Ogata, K. (2002). *Modern Control Engineering* (4th ed.). Upper Saddle River, New Jersey: Prentice Hall.
- [8] PerceptiVU, Inc. Retrieved October 18, 2005, from <http://www.perceptivu.com/TargetTrackingSoftware.html>
- [9] Siouris, G. M. (1993). *Aerospace Avionics Systems: A Modern Synthesis*. New York: Academic Press.
- [10] Solid State 3-axis Pitch, Roll, & Yaw Sensor. Retrieved October 29, 2005, from <http://www.microstrain.com/3dm.aspx>
- [11] Van Doren, V. J. (2001, April 1). *Overcoming the deadtime dilemma*. Retrieved October 18, 2005, from <http://www.manufacturing.net/ctl/index.asp?layout=articlePrint&articleID=CA186211>

- [12] Wang, I. H., Dobrokhodov, V. N., Kaminer, I. I., & Jones, K. D. (2005). On Vision-Based Target Tracking and Range Estimation for Small UAVs. *American Institute of Aeronautics and Astronautics*. Retrieved December 05, 2005, from http://pdf.aiaa.org/preview/CDReadyMGNC05_1089/PV2005_6401.pdf

INITIAL DISTRIBUTION LIST

1. Defense Technical Information Center
Ft. Belvoir, Virginia
2. Dudley Knox Library
Naval Postgraduate School
Monterey, California
3. Dr. Anthony J. Healey
Naval Postgraduate School
Monterey, California
4. Dr. Isaac I. Kaminer
Naval Postgraduate School
Monterey, California
5. Dr. Vladimir N. Dobrokhodov
Naval Postgraduate School
Monterey, California